

Petrographic and geochemical properties of the ignimbrites around Hatunsaray (Konya)

Hacer Bilgilioğlu¹, Halil Baş²

¹Aksaray University, Faculty of Engineering, Department of Geological Engineering, Aksaray, Turkey

²Konya Technical University, Faculty of Engineering, Department of Geological Engineering, Konya, Turkey

Keywords

Hatunsaray
Ignimbrites
Petrography
Geochemistry

ABSTRACT

The study area is located around the town of Hatunsaray, approximately 40 km away from the south-west of Konya. In this study, the petrological and geochemical characteristics of the Bulumya ignimbrite, Detse ignimbrite and Sadıklar ignimbrite observed in the region were revealed. The study area contains Upper Miocene - Lower Pliocene aged Güneydere formation and overlying Bulumya ignimbrite, Detse ignimbrite, Sadıklar ignimbrite and Quaternary alluviums. All these units were formed in the Upper Miocene - Lower Pliocene aged fluvial and lake environment and have a lateral vertical transition with carbonate, clastic units. The gray-colored Bulumya ignimbrite contains andesite-dacite rock fragments and large pumice grains. The Detse Ignimbrite is yellow in color and shows a well sorted lapilli tuff composition. The Sadıklar Ignimbrite, on the other hand, contains agglomeratic levels with yellow colored slightly fused lenses and wedge geometry. All ignimbrite samples have porphyric texture and were classified as "crystal-vitric tuff" and "crystal lithic-vitric tuff" in the glass-crystal-rock fragment classification. Petrographic investigations of ignimbrites show that major components are quartz, plagioclase, plagioclase microliths, biotite, amphibole, opaque minerals and rock fragments. Geochemical data shows that all ignimbrite samples are subalkaline, trachy-andesite, andesite-basaltic andesite and calc-alkaline in character. When the main oxide, trace and rare earth elements in ignimbrites are evaluated, fractional crystallization controlled by feldspar minerals is observed. In addition, the high K and Rb content in the spider diagrams indicate crustal contamination. The distribution of the ignimbrite samples in the Rb/Y-Nb/Y diagram suggests that the magma source forming the samples is enriched by subduction and/or crustal components.

1. INTRODUCTION

Extensive volcanic activity in Turkey developed as a result of the Arabian plate colliding with the Eurasian Plate before the Miocene. With this collision, which marked the beginning of the Neotectonic period, the formation of the East and North Anatolian faults began. The Anatolian block started moving westward along these two major faults, and widespread volcanic activity in the Neotectonic period occurred (McKenzie, 1972; Şengör et al., 1985; McKenzie and Yılmaz, 1991). Depending on these activities, volcanic rocks covered an area of approximately 85,000 km² in Eastern, Central and Western Anatolia. The predominantly calc-alkaline volcanic products located in the west of Konya covering large areas

(Figure 1). Surrounded by the North Anatolian Fault in the north and the African-Anatolian convergence system in the south, this area is considered to have developed under transtensive and transpressive tectonic regimes that have been effective since the Late Miocene (Şengör et al., 1985; Kempler and Garfunkel, 1991) (Figure 1). According to Keller et al., (1977), volcanic activity in this area continued from the Late Miocene (11.9 Ma) to the Pliocene (3.35 Ma). A limited number of studies have been conducted on these volcanics around Konya (Ota and Dinçel, 1975; Keller et al., 1977; Ulu et al., 1994; Kurt et al., 2003; Koçak, 2012; Asan and Ertürk, 2013; Uyanık and Koçak, 2016; Koçak, 2017; Koçak, 2021). Petrological and geochemical data obtained from volcanic rocks provide information about the geodynamics of the study area. The aim of this study

* Corresponding Author

¹(hcanbas@aksaray.edu.tr) ORCID ID 0000-0002-8629-1077
(hbas@selcuk.edu.tr) ORCID ID 0009-0007-8686-780X

Cite this article

Bilgilioğlu, H., & Baş, H. (2023). Petrographic and geochemical properties of the ignimbrites around Hatunsaray (Konya). Turkish Journal of Geosciences 4(1), 13-28.

Received: 10/03/2022; Accepted: 10/04/2023

is to characterize the petrological and geochemical properties of ignimbritic rocks in the Konya (Hatunsaray) region and to interpret the origin of magmas. In the vicinity of the study area, the basement rocks form an ophiolitic complex with pre-Miocene schist, marble, quartzite, and dolomitic limestones (Eren, 1993; Koçak and Kaya, 2019). Volcanic, volcano-sedimentary units and lacustrine and fluvial sediments unconformably overlie these units (Keller et al., 1977; Ulu et al., 1994; Temel et al., 1995; Temel et al., 1998). Neo-autochthonous units follow a regional angular unconformity on the autochthonous and allochthonous paleotectonic formations in the region. These units belonging to the Late Miocene-Early Pliocene aged Dilekçi group formed in the neotectonic period begin with the Ulu Muhsine formation, which is composed of lacustrine limestones and marls at the bottom. The Küçük Muhsine formation, which includes tuff-tuffite-volcanic breccia and sandy-muddy clastics, is conformably observed in the Ulumuhsine formation. Erenlerdağı volcanics formed by lava flows of dacitic-andesitic composition overlie the Küçük Muhsine formation. On the other hand, the Plioquaternary aged, horizontally bedded,

diagenetic conglomerate, sandstone, mudstone Topraklı formation overlies the lacustrine, volcano-sedimentary and volcanic faces units forming the Dilekçi group with an angular unconformity. All these units are covered by Quaternary alluvium, especially around Hatunsaray (Turan et al. 1997; Soğucaklı, 2006). The geology of the study area and its surroundings has been studied by Göğür and Kırıl (1973), Özcan et al. (1990) and Ulu et al. (1994) and many researchers. Keller et al. (1977) and Temel et al. (1995) conducted studies on the geology, petrology and geochemistry and radiometric dating of the volcanics in the region. According to Keller et al. (1977), the age of the rocks was found to be 11.95-3.35 Ma by fossil content and radiometric dating method. In the study, ignimbrites cropping out in the region were examined under four different names: Kızılören ignimbrites, Erenkaya (Bulumya) ignimbrites, Detse (Kuzagıl) ignimbrites and Sadıklar ignimbrites. This study aims to approach the origin of ignimbrites by determining the petrographic and geochemical properties of Bulumya (Erenkaya) ignimbrites, Detse (Kuzagıl) ignimbrites and Sadıklar ignimbrites.

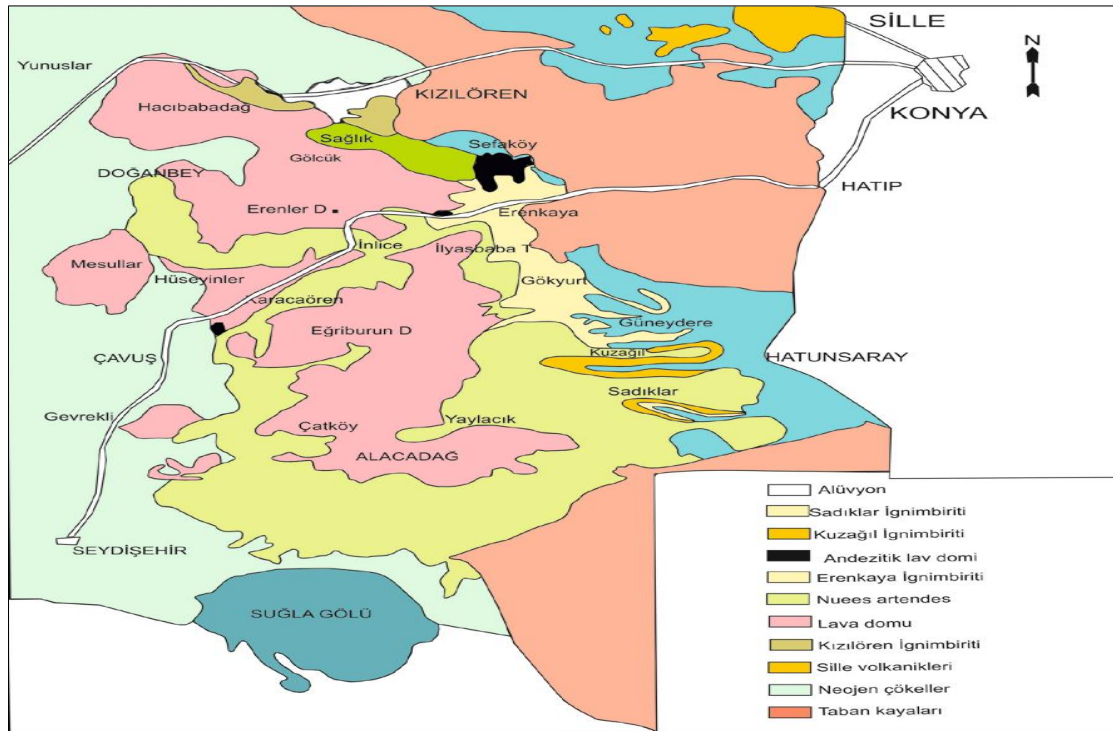


Figure 1. A regional geological map (Keller et al., 1977).

2. METHOD

Within the scope of the study, the stratigraphic relations of the units with each other were examined, and samples were taken for petrographic and geochemical investigations in the study area (Figure 2). Thin sections made for petrographic and mineralogical examinations were examined under polarizing microscope. These examinations were

carried out in the Aksaray University Geological Engineering Optical microscope laboratory. The mineralogical, petrographic and textural properties of the rocks examined under the polarizing microscope were determined. According to petrographic examinations, main oxide, trace and rare earth element analyzes were made from the least altered samples. The samples were ground to approximately 200 mesh first in a jaw grinder and

then in a ring grinder, were sent to ACME Analytical Laboratories for major oxide, trace and rare element analysis. Here, major oxide and trace elements were

analyzed by X-Ray Diffractometry (XRD) and rare earth elements were analyzed by ICP-MS (Inductively coupled plasma-mass spectrometer).

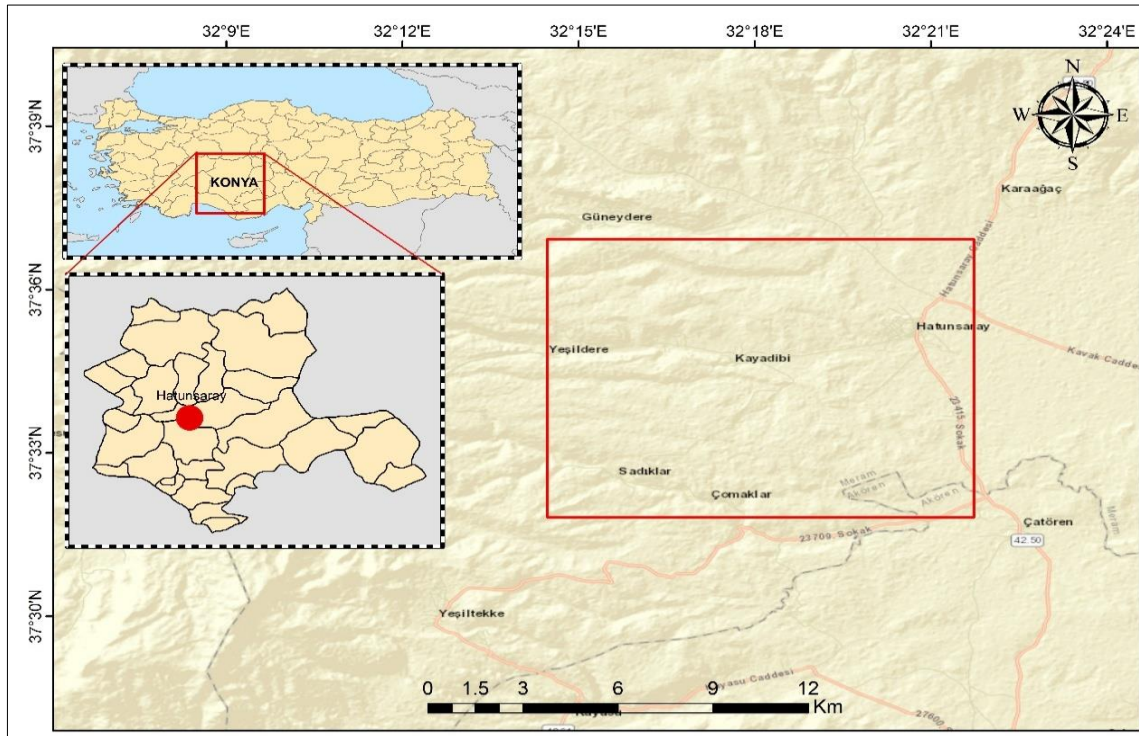


Figure 2. Study area.

3. RESULTS

3.1. General Geology

The Upper Miocene - Lower Pliocene aged Dilekçi group forms the basis of the units in the study area. The unit was named "Dilekçi formation" for the first time by Göğer and Kırıl (1969). These units were later subdivided by Eren (1993) under the name of the Dilekçi group as Sille formation, Ulu Muhsine formation, and Küçük Muhsine formation. Since this study focuses on the petrographic and petrological characteristics of the ignimbrites in the region, no formation distinction was made in the clastics and carbonates in the Dilekçi group and they were examined as a single formation as the Güneydere formation. The Güneydere formation is Upper Miocene-Lower Pliocene aged and includes Bulumya ignimbrite, Detse ignimbrite, Sadıklar ignimbrite, Explosion breccia and nuée ardente (Glowing cloud) members from bottom to top. Alluviums consisting of loose sediments overlies these units unconformably.

3.1.1. Bulumya Ignimbrite

The Bulumya ignimbrite, named for the first time by Keller et al. (1977), consists of grey-coloured

ignimbrites formed as two separate eruption phases. A nearly horizontal paleosol zone separated these two phases with an inclination of 0-5 degrees towards the south. In the lower levels of ignimbrite, massive, poorly sorted, thickness varying laterally according to topography, less fused, less crystalline, pumice-predominant andesite, basalt dacite rock fragments are observed in approximately 25 m thick. In the upper levels, it has a better fused, coarse and polycrystalline grain structure compared to the lower level. Both levels in the Bulumya ignimbrite have the same composition in terms of both chemical and mineral presence, and it has been determined that they are successive cooling units (Keller et al., 1977). Below the unit, pyroclastic surge deposits are located in lateral vertical transitions with clastic carbonate units, where these deposits are absent (Figure 3). Above it, Detse ignimbrite and Sadıklar ignimbrite overlain by eruption breccia and accompanying units where these units are not present. The age of the Bulumya ignimbrite was determined as 9-9.4 my in the age determination made by the K/Ar method by Keller et al. (1977).

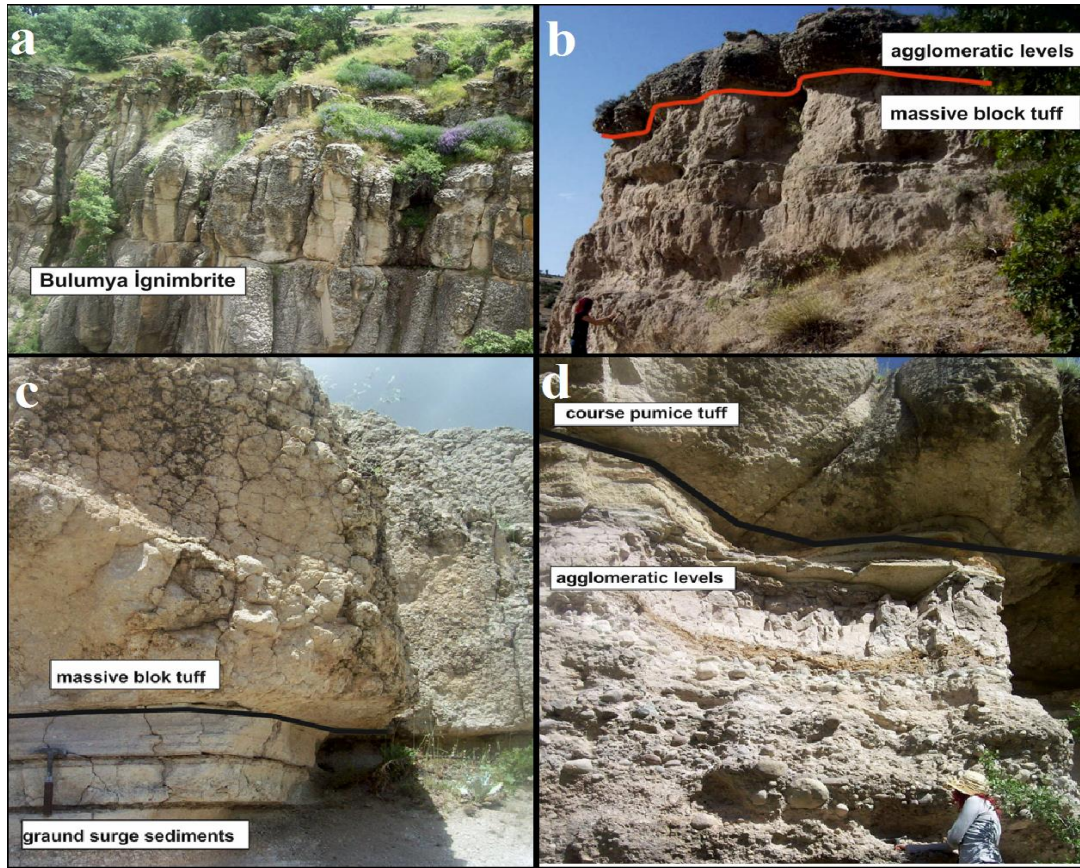


Figure 3. Bulumya Ignimbrite a) separation of the lower and upper levels by the paleosol level b) agglomeratic levels and tuff boundary view with massive blocks c) with massive block tuff and ground surge sediment d) course pumice tuff and agglomeratic levels.

3.1.2. Detse Ignimbrite

Detse ignimbrite is a yellow-colored lapilli tuff with well-sorted lower levels. This unit, which contains coarse pumice grains, andesite, dacite and basalt rock fragments towards the top, has a laterally variable thickness. It is thick, where the topography on which it flows is pits, and thin, where there are bumps. There are lens and wedge-shaped agglomeratic levels in places within the unit. In the lower levels of Detse ignimbrite, it has a massive, unbedded, tabular and occasionally irregular

geometry. It contains andesite, dacite and basalt rock fragments in pumice and lapilli size. It is poorly sorted and the grains are supported by tuff matrix. In the upper parts, agglomeratic levels with lens and wedge geometry are dominant. It is a medium round, poorly sorted, consisting of andesite, dacite, basalt and pumice blocks (Figure 4). Bulumya ignimbrite is overlain by the Detse ignimbrite stratigraphically. Where Bulumya ignimbrite is not observed, it is laterally and vertically transitional with clastic and carbonate units. This unit is covered by the eruption and flow breccia and accompanying units.

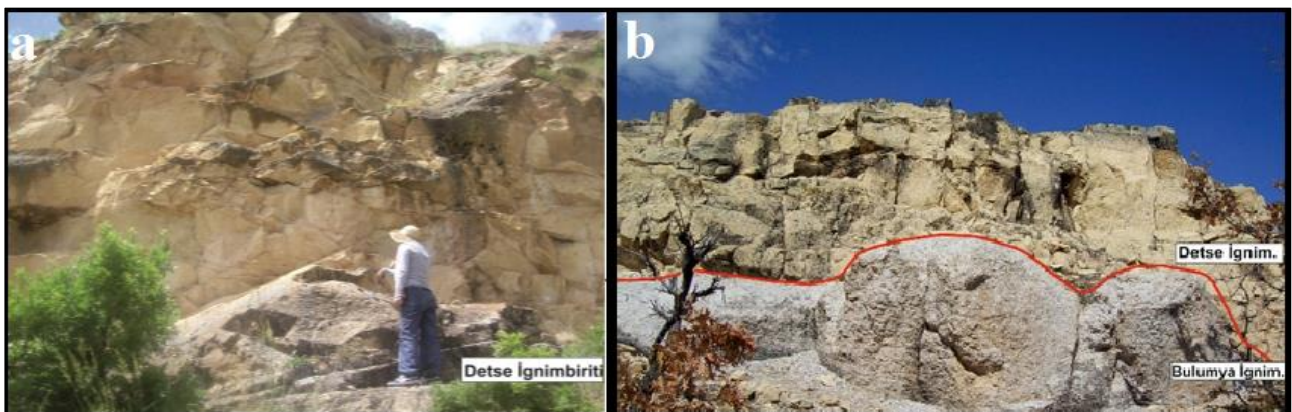


Figure 4. Detse Ignimbrite a) land view b) Bulumya ignimbrite border relation

3.1.3. Sadıklar Ignimbrite

Sadıklar ignimbrite generally contains yellow-colored, less fused, agglomeratic layers with lens and wedge geometry. In its upper levels, there are dust cloud surge deposits. Sadıklar ignimbrite is mostly homogeneous, fine-grained, sometimes ignimbritic tuff containing andesite pebbles. The approximate thickness of the unit is around 50 m. Sadıklar ignimbrite continues with a pink-colored fine-grained tuff level above the lapilli tuff levels

containing agglomeratic levels at the bottom. Bulumya ignimbrite is located stratigraphically under the Sadıklar ignimbrite. Where the unit is not observed, it is laterally and vertically transitional with clastic and carbonate units. The lower level of the Sadıklar ignimbrite consists of lens-shaped, coarse-grained tuff layers. This level contains coarse tuff grains and fine lapilli with lens and wedge geometry and shows reverse gradation from place to place. Thick-bedded, poorly sorted, massive lapilli tuffs are observed over this unit (Figure 5).

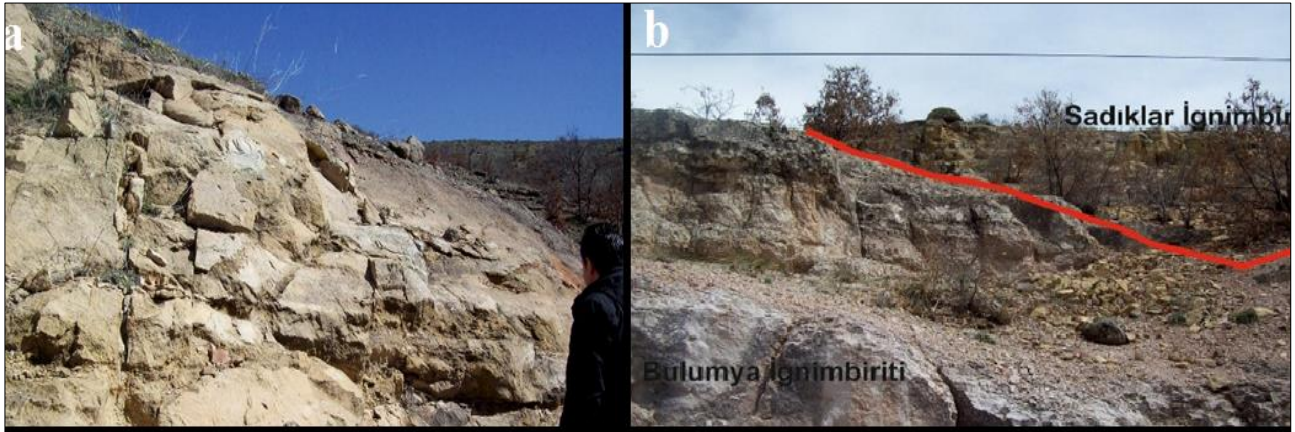


Figure 5. Sadıklar ignimbrite a) land view, b) Bulumya ignimbrite border relation.

3.1.4. Explosive breccia, nuée ardente and associated continental deposits

Named for the first time by Keller et al. (1977), this unit spreads over a very wide area in the study area and the region. This unit consists of agglomerate, red-brown colored tuff, conglomerate, sandstone, siltstone and lava alternation. The unit is approximately 50 m thick and laterally transitions to conglomerate, sandstone and sometimes lacustrine limestones (Ulu et al., 1994). In the age determination, it is stated that the age of the unit is 5.76 Ma. According to this data, the age of the unit is Upper Miocene – Lower Pliocene. The Detse ignimbrite and the Sadıklar ignimbrite are located under the unit. Alluvial deposits are unconformably overlying the unit.

3.2. Petrography

In the geological literature, the term ignimbrite was first used by Marshall (1935) to describe Taupo tuffs with acidic composition, which are widely spread and welded in some places. The definition of ignimbrite is made in different ways by different researchers. In these definitions, the term ignimbrite is sometimes used to describe a lithological unit corresponding to welded tuff. Sometimes it is used to mean a sediment formed as a result of pyroclastic flows. According to Sparks et al. (1973), ignimbrite is defined as "a special type of pyroclastic flow deposits containing abundant pumice, volcanic glass splinters, regardless of volume and degree of

welding". McPhie et al. (1993) define it as "rocks formed by the combination of pumice fragments ranging in size from bomb to lapilli size and lesser lithic fragments by a matrix composed of vitric, crystal and lithic ash". Ignimbrites result from the collapse of an eruption column of a single explosion or a series of successive eruptions. As a result of the collapse of Plinian eruption columns, large volumes of pumice flows with abundant pumice occur. The pyroclastic material deposited from the Plinian eruption column flows along the surface due to gravity and is deposited in one place. Such flow deposits are defined as ignimbrite. Generally, the topography that fills the valley and depression areas shows controlled settlement (Cas and Wright, 1988).

The ignimbrites around Konya have been studied by many researchers (Göğür and Kırıl, 1973; Özcan et al., 1990; Ulu et al., 1994; Keller et al., 1977; Temel et al., 1995). In these studies, ignimbrites cropping out in the region were studied under four different names: Kızılören ignimbrites, Erenkaya (Bulumya) ignimbrites, Detse (Kuzagıl) ignimbrites and Sadıklar ignimbrites. This study aims to approach the origin of ignimbrites by determining the petrographic and geochemical properties of Erenkaya (Bulumya) ignimbrites, Detse (Kuzagıl) ignimbrites and Sadıklar ignimbrites. The petrographic features of the Bulumya, Deste and Sadıklar Ignimbrites identified in the study area were revealed from the thin sections. In petrographical studies, the main mineralogical composition of ignimbrite samples was determined as quartz + plagioclase + plagioclase microliths +

biotite + amphibole + sericite + iron oxide + opaque mineral + volcanic glass + lithic component. Ignimbrites show a hypocrySTALLINE porphyritic texture. In petrographical studies, the main mineralogical composition of ignimbrite samples was determined as quartz + plagioclase + plagioclase

microliths + biotite + amphibole + sericite + iron oxide + opaque mineral + volcanic glass + lithic component. Ignimbrites show hypocrySTALLINE porphyritic texture according to the grain state (Table 1).

Table 1. Mineral compositions of ignimbrite samples detected in microscopic examinations.

Sample	Q	Plg	Plg Mic.	Bi	Ser.	Op	Fe	Volc. Glass	Lytic comp.	Name of the rock
B1	+	+	+	+	+	+	+	+	-	Crystal-vitric tuff
B2	+	+	+	+	+	+	±	+	-	Crystal-vitric tuff
B3	+	+	+	+	+	+	±	+	-	Crystal-vitric tuff
B4	+	+	+	+	+	+	±	+	-	Crystal-vitric tuff
B5	+	+	+	+	+	+	+	+	-	Crystal-vitric tuff
B6	+	+	+	+	+	+	+	+	+	crystal lithic vitric tuff
B7	+	+	+	+	+	+	+	+	+	crystal lithic vitric tuff
B8	+	+	+	+	+	+	±	+	-	Crystal-vitric tuff
D1	+	+	+	-	+	+	+	+	-	Crystal-vitric tuff
D2	+	+	+	-	+	+	+	+	-	Crystal-vitric tuff
D3	+	+	+		+	+	+	+	+	crystal lithic vitric tuff
D4	+	+	+	±	+	+	+	+	-	Crystal-vitric tuff
D5	+	+	+	-	+	-	-	+	-	Crystal-vitric tuff
D6	+	+	+	±	+	+	-	+	-	Crystal-vitric tuff
D7	+	+	+	-	+	+	+	+	-	Crystal-vitric tuff
D8	+	+	+	-	+	+	+	+	-	Crystal-vitric tuff
S1	+	+	+	-	+	+	±	+	-	Crystal-vitric tuff
S2	+	+	+	-	+	+	+	+	-	Crystal-vitric tuff
S3	+	+	+	-	+	+	+	+	-	Crystal-vitric tuff
S4	+	+	+	-	+	+	+	+	-	Crystal-vitric tuff
S5	+	+	+	-	+	+	±	+	-	Crystal-vitric tuff
S6	+	+	+	-	+	+	±	+	-	Crystal-vitric tuff
S7	+	+	+	-	+	+	+	+	+	crystal lithic vitric tuff
S8	+	+	+	-	+	+	+	+	+	crystal lithic vitric tuff

(Q; quartz, San; sanidine, Pl; plagioclase, Bi; biotite, Kal; Ser; serizite, Op; opaque mineral, Fe; iron oxide mineral)

In addition, vitrophyric texture, microcrystalline texture, poikilitic texture, glass splinters and pumice fragments were found in the ignimbrites. In the microscopic examination of the samples, sericitization, iron oxidation, opacitization, and chloritization type alterations are observed. Quartz in ignimbrites has been determined as different sizes and coarse-grained, and resorbing and fractures in quartz are noteworthy. Biotites are known as euhedral to subhedral, dark brown. In addition, there are bending, twisting and fractures in biotite. Alterations such as chloritization, iron oxidation and opacification have been observed in

the biotites. Plagioclase minerals observed in different sizes, show polysynthetic and zonal extinction, and it has been calculated that they have oligoclase and andesine characteristics based on their extinction angle. Plagioclase minerals mostly show sericitization and argillization type weathering according to the matrix (Figure 6). The ignimbrite samples were determined as "vitric tuff" in the classification of Schmid (1981) considering the glass-rock fragment-crystal components. In the classification made according to Carozzi (1993), the examined samples range from crystal vitreous tuff to crystalline lithic vitric tuff.

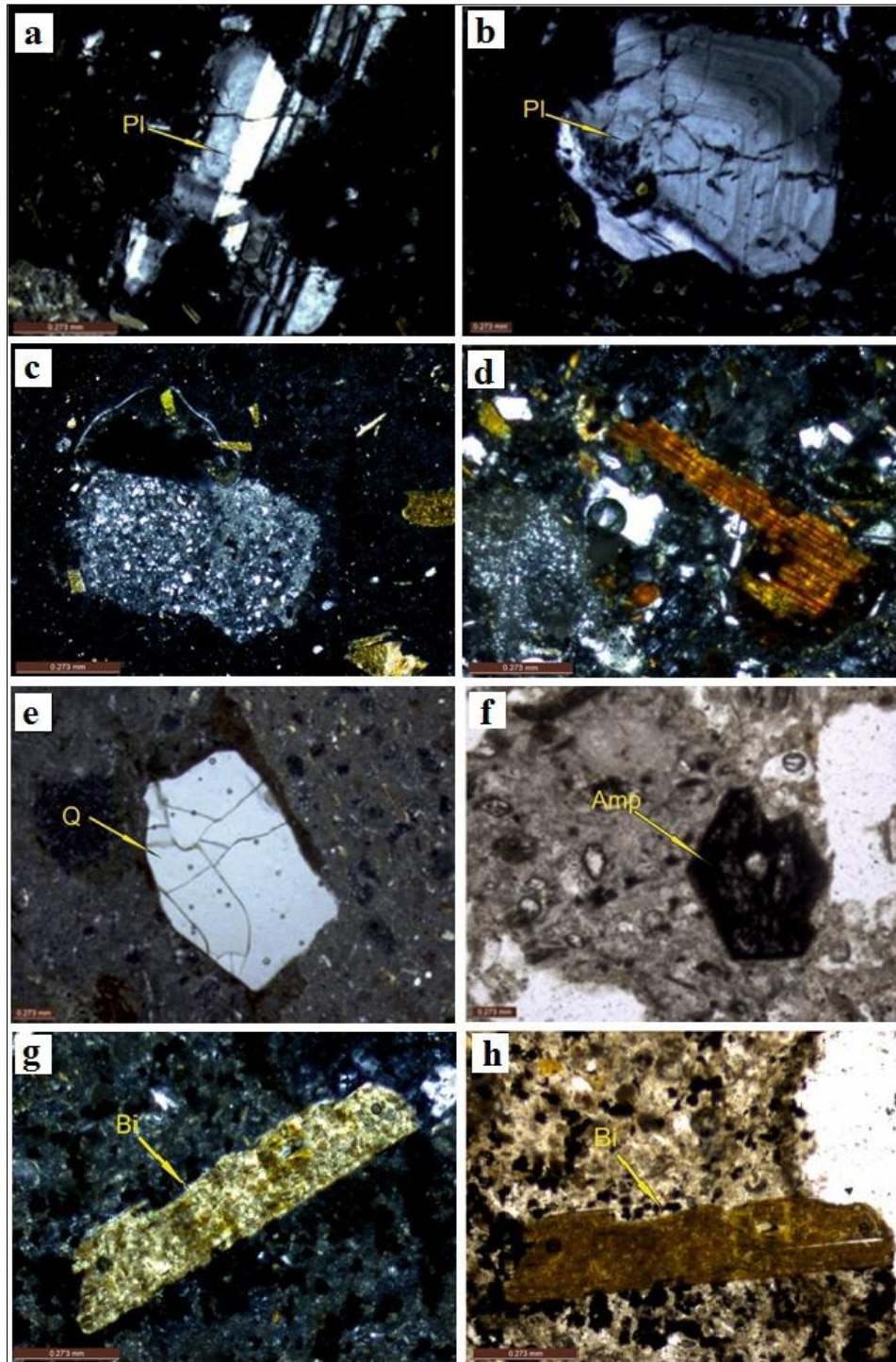


Figure 6. Ignimbrite samples a) Polysynthetic twinned plagioclase (double nicol) b) zoned plagioclase (single nicol) c) sericitization type alteration (cross nicol) d) resorbed edges biotite mineral (double nicol) e) significant fractures in the quartz mineral (double nicol) f) opacified amphibole g) biotite mineral (double nicol) h) biotite mineral (single nicol).

3.3. Geochemistry

3.3.1. Major and Trace Element Geochemistry

Major, trace and rare earth element analyses were carried out to determine the geochemical properties of the ignimbrite samples. The analysis results were interpreted using different diagrams, and the character and chemical properties of the

magma forming the ignimbrites were constrained. In the samples, Al_2O_3 content varies between 5.31%-21.31%, SiO_2 53.16%-75.39%, MgO 0.01-1.09%, $Fe_2O_3^*$, 0.01-5.55%, TiO_2 0.43-0.82%, CaO 0.08-2.6%, Na_2O content 0.03-1.63%, K_2O It varies between 1.31-4.22, P_2O_5 0.08-0.86%, MnO 0.01-0.05% according to the matrix. The geochemical analysis of the ignimbrite samples is given in Table 1 and 2.

Table 2. Major oxide analyses of the ignimbrites.

Sample	SiO ₂ %	TiO ₂ %	Al ₂ O ₃ %	Fe ₂ O ₃ %	MnO %	MgO %	CaO %	Na ₂ O %	K ₂ O %	P ₂ O ₅ %	LOI %	TOTAL %
S5	73,99	0,67	8,42	0,01	0,01	0,01	0,08	0,03	1,66	0,3	15,9	101,08
S6	71,31	0,78	8,33	0,01	0,01	0,01	0,13	0,13	2,29	0,19	16,2	99,38
S7	57,68	0,66	21,19	0,02	0,02	0,01	0,16	0,09	4,22	0,86	17,01	101,86
S9	62,02	0,65	9,08	0,5	0,03	0,5	0,48	0,47	3,43	0,23	20,6	97,99
D2	73,1	0,74	6,86	0,1	0,01	0,1	0,27	0,32	2,17	0,35	15,7	99,72
D3	68,19	0,8	11,73	0,08	0,02	0,08	0,22	0,35	2,87	0,82	14,2	99,36
D5	75,39	0,82	5,31	0,37	0,02	0,37	0,48	0,16	1,31	0,22	15,8	100,25
D6	71,77	0,81	6,72	0,19	0,01	0,19	0,29	0,79	2,8	0,29	16,3	100,16
D8	72,37	0,55	7,56	0,15	0,03	0,15	0,63	0,45	2,11	0,85	14,3	99,15
B2	60,35	0,63	8,86	3,09	0,04	1,09	1,67	1,23	2,12	0,08	19,1	98,26
B3	60,49	0,56	6,02	4,81	0,05	0,81	0,98	0,71	1,9	0,68	20,2	98,21
B4	59,63	0,59	8,53	5,02	0,04	1,02	1,58	1,13	2,11	0,08	18,3	98,3
BI6	55,16	0,59	21,31	5,55	0,04	0,9	1,01	0,83	1,97	0,84	11,9	100,1
BI8	58,77	0,63	18,54	5,43	0,04	0,87	2,61	1,63	2,18	0,16	10,2	101,06

Table 3. Trace element results of ignimbrites.

Samp.	Sc	Ba	Cs	Ga	Hf	Nb	Rb	Sr	Ta	Th	U	V	W	Zr	Y	Cu	Pb	Zn	Ni	As	Au
	ppm	ppm	ppm	ppm	ppm	ppm	ppm	ppm	ppm	ppm	ppm	ppm	ppm	ppm	ppm	ppm	ppm	ppm	ppm	ppm	ppm
S3	13	1211	12,4	62,9	6,6	18,6	42,5	1408,5	1,3	33,5	6,2	413	3,1	212,7	5	12,8	101,5	26	0,9	161,9	3,4
S5	3	969	3,2	40,6	3,8	13,8	8,5	272,7	1,1	17,8	5,1	231	3,8	129,9	2,1	2,5	244,7	17	0,5	73	1,1
S6	5	1014	9,3	22,7	5,7	13,5	37	234,2	1,2	11,1	2,2	143	2,8	201,1	1,5	3,7	159,1	15	0,5	47,1	2,2
S7	5	1347	1,7	25,2	5,1	12	19,3	969,3	1	34,2	2	186	1,9	178,8	1,9	2,7	1325,2	10	0,6	329,6	<0,5
S9	45	769	15,5	18,3	3	9,5	78,6	1162,5	0,5	18,1	4,4	365	2,4	137,1	3,8	15	18,3	83	5,8	14,8	<0,5
D2	10	923	4,7	10,4	5,5	12,3	43,4	800	0,8	29,5	4,5	78	1,8	196,5	6,6	4,4	142,1	14	0,9	36,3	3,6
D3	11	1262	4,7	27,2	5,5	13,3	38,7	1706,6	0,9	36,7	5,2	224	2,2	191,2	8,3	5,6	57,8	15	0,6	66,5	2,8
D5	7	718	8,2	23,6	6,9	16,7	40,7	604	1,6	19,3	5,4	168	3,5	256	6,3	12	22,2	40	4,6	8,5	3,1
D6	6	1281	3,5	8,1	5,1	13,6	48,1	404,4	0,8	28,8	5,1	91	2,1	200,8	6,1	3,2	30,4	6	0,3	37,7	1,6
D8	8	1785	5,6	21,1	3,4	9,1	59,3	2539,6	0,4	75,2	5	207	1,4	131,9	11	16,1	13,8	35	1,8	19	1,3
B2	16	684	13,4	15,3	5,4	10,1	109,4	474,9	0,7	15,3	6,7	118	1,7	190,9	14,1	25,3	16,9	54	4,7	1,5	7,6
B3	9	922	10,1	19,9	4	10,2	113	2307	0,7	19,8	6,6	137	0,6	159	15,6	14,8	9,5	46	2,5	1,3	1,2
B4	15	680	12,3	15,1	4,3	10,4	109	471	0,8	16,1	6,3	105	1	160	13,4	22,1	15,8	50	3,9	1,2	3,2
BI6	12	1191	12,6	17,3	5,8	11,8	109,8	2834,1	0,8	21,7	8,6	124	1,9	212,4	21,7	25,2	9,7	45	3,4	2,5	1,9
BI8	12	769	7,8	17,4	4,1	10	98,8	747,8	0,8	16,6	8,7	120	1,8	152,7	33,5	29,6	13,4	100	4,8	0,8	13,8

According to the analysis results of the ignimbrite samples, a total alkali (%Na₂O+ K₂O) - silica (%SiO₂) diagram was prepared to determine the character of the magma, and it was determined that the samples placed in this diagram fell into the subalkaline area (Figure 5a). The ignimbrite samples showing a subalkaline magma character were collected in the calc-alkaline area in the AFM diagram developed by Irvine and Baragar (1971) (Figure 5b). Examples are located in the high-K calc-alkaline series and Calc-alkaline series areas in the SiO₂ vs. K₂O diagram (Peccerillo and Taylor, 1976). It is known that the K calc-alkaline boundary of the K₂O-SiO₂ diagram is a feature that reflects the active continental margin and continental orogenic

regions. In addition, samples with high alkali properties show high values in the orogenic series of large ion lithophile elements (e.g. K, Rb, Ba, Sr and Zr). Elements such as Zr, Nb, Y, TiO₂, which are known to be stable against chemical events such as alteration, metamorphism and metasomatism, are frequently used especially in nomenclature of the volcanic rocks, determining their petrological properties and tectonic formation environments. In the Nb/Y-Zr/TiO₂*0.0001 rock naming diagram (Pearce, 1996), created by using Nb, Y, Zr and TiO₂ elements, the samples are mostly found in trachy-andesite, andesite - basaltic andesite areas according to the matrix (Figure 7).

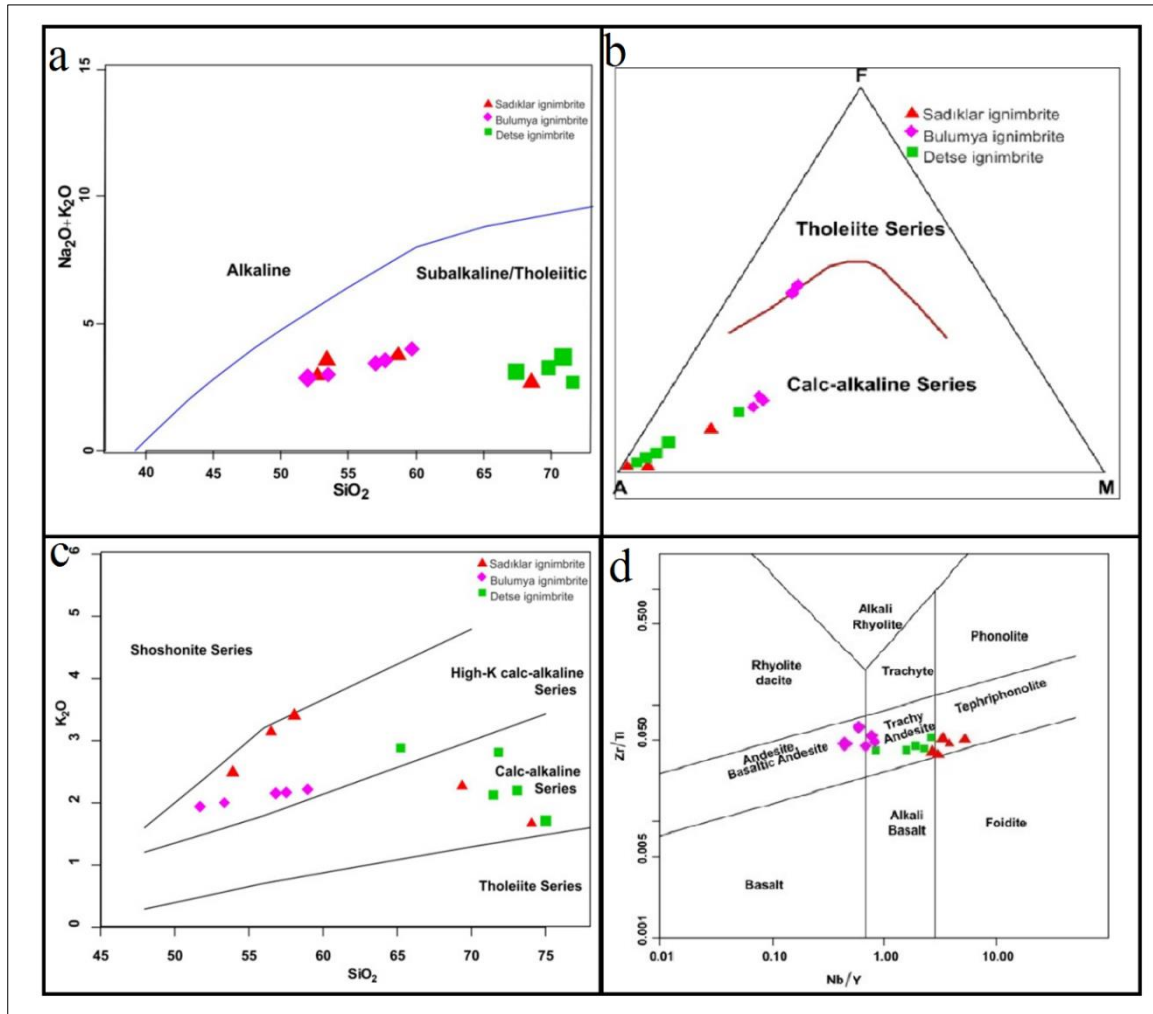


Figure 7. Nomenclature diagrams of the ignimbrite samples a) $\text{SiO}_2(\%)$ - $\text{Na}_2\text{O}+\text{K}_2\text{O}(\%)$ (Irvine and Baragar, 1971), b) AFM diagram (Irvine and Baragar 1971) c) $\text{SiO}_2(\%)$ - $\text{K}_2\text{O}(\%)$ diagram (Peccerillo and Taylor, 1976) d) Nb/Y - $\text{Zr}/\text{Ti} \times 0.0001$ diagram (Pearce, 1996).

Harker diagrams were made to examine the behaviour of major and trace elements against SiO_2 . No coherent variations were observed in the variation diagrams prepared by using the main oxide and trace element contents of the ignimbrite samples against SiO_2 . In the main oxide element change diagrams of the samples, it is seen that MgO , Fe_2O_3 , Al_2O_3 and CaO elements show a negative trend as SiO_2 amount increases. Also, in harker diagrams, the Bulumya samples differ from other samples and exhibit better correlations; SiO_2 contents increase with increasing CaO , Na_2O and K_2O . This can be explained by the reduction of MgO , Fe_2O_3 , Al_2O_3 and CaO elements by incorporating them into anorthite-rich plagioclase (Ca plagioclase), amphibole, biotite

and opaque minerals (magnetite, titanomagnetite). The negative correlation with Al_2O_3 indicates the plagioclase fractionation in the development of ignimbrite samples. As the amount of SiO_2 increases, a positive increase is observed in the amount of Na_2O . The observed positive increase in Na_2O can be explained by the incorporation of Na into the minerals formed later. In addition, against SiO_2 , MgO , CaO and Fe_2O_3 with the increase of SiO_2 indicates the fractionation of magnetite and titanomagnetite (Fe-Ti oxides). The reduction in MgO content probably associated with the clinopyroxene fractional while the reduction in Fe_2O_3 content be associated with the pyroxene and Fe-Ti oxide fractionation (Figure 8).

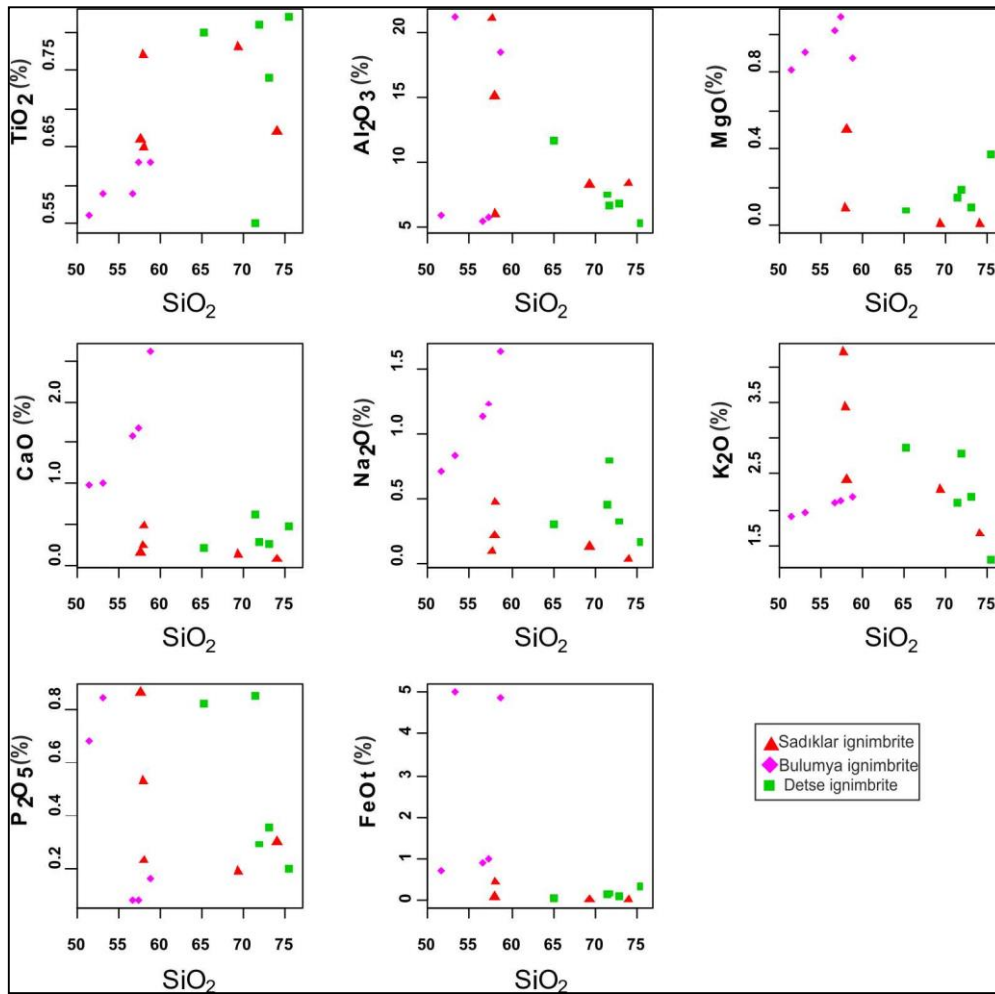


Figure 8. Main oxide element variation diagrams of ignimbrite samples versus SiO₂.

It is seen that, in the trace element results of the ignimbrite samples examined in general, the large ion lithophile (LIL) element (K, Sr, Rb, Ba) amounts were higher than the high field strength (HFS) elements (Y, Hf, Zr, Ti, Nb). According to these diagrams, there is a negative relation between incompatible elements such as Rb and Ba and SiO₂, and a positive relation between compatible elements such as Sr and Nb. As the silica content increases, the incompatible element contents increase and the compatible element contents decrease, which is explained by fractional crystallization. It indicates that the rocks with these changes in the main oxide and trace elements may have been derived from the main magma by fractional crystallization. It is thought that the rocks with these changes in the main oxide and trace elements may have been derived from the main magma by fractional crystallization. However, the main magmatic event

in the development of these rocks is not thought to be the effect of other magmatic events. (magma mixing, crustal contamination, etc.) The positive correlation of incompatible element K₂O against SiO₂ and increases in incompatible elements indicate that they are enriched probably due to crustal contamination and alteration. Since K-containing minerals (K-feldspar and biotite) are the last crystallized products in the magmatic melt, an increase is observed in the Rb element in parallel with the increase in SiO₂. The first increase and then decrease in Ba content against SiO₂ indicates the formation of sanidine in rhyolite-type tuffs (Rollinson, 1993). Since Hf and Zr elements have similar ion radii, they act together in the magmatic system. Zr is seen in large amounts in the last crystallized products during crystallization according to the matrix (Figure 9).

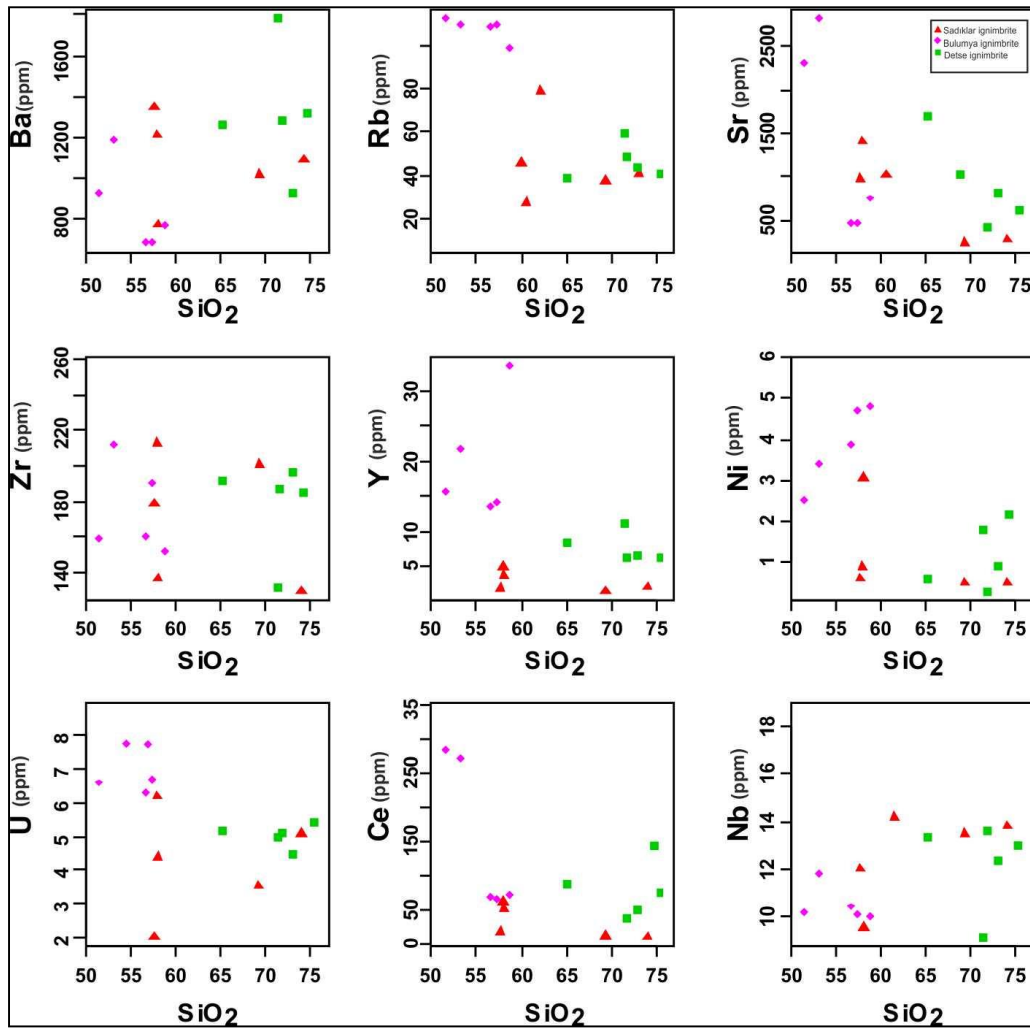


Figure 9. Trace element variation diagrams of ignimbrite samples versus SiO₂.

The main magma was tried to be determined by drawing the trace element distributions of the samples normalized according to the primary mantle and chondrite. When looking at the spider diagrams normalized to the Primary Mantle, a significant lithophile element enrichment with a large ion radius and significant negative anomaly are observed in elements with high persistence. In the fractional crystallization process, the presence of positive anomalies in Sr and Ba elements shows the effect of feldspar minerals, and the presence of positive anomalies in Ti element (except for Bulumya samples) shows the effect of Fe-Ti oxide minerals. While the enrichment in K, Rb and Th elements may have resulted from crustal

contamination, the presence of Nb anomaly indicates the effect of subduction and/or crustal components on the development of the main magma of the volcanic. When we look at the chondrite normalized spider diagrams, it is noteworthy that a lithophile element with a significantly large ion radius and elements with high enrichment and persistence, Pb, P and Ti are also consumed in REEs with significant negative anomalies. Lithophile element enrichment may result from continental crustal contamination. Excessive enrichment of rocks (especially K, Rb and Th) in terms of large ion lithophile elements (LILE) and depletion in terms of Nb and Ti are characteristic features observed in trace element distributions according to the matrix (Figure 10 and Figure 11).

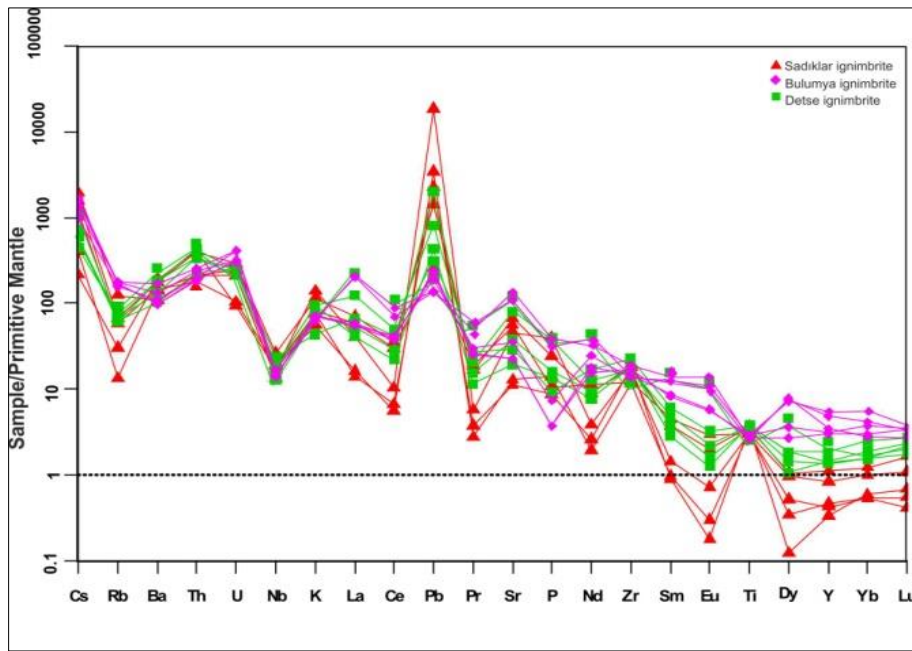


Figure 10. Examples of multi-element distributions normalized to the primary mantle (Normalization values, Sun and McDonough, 1989).

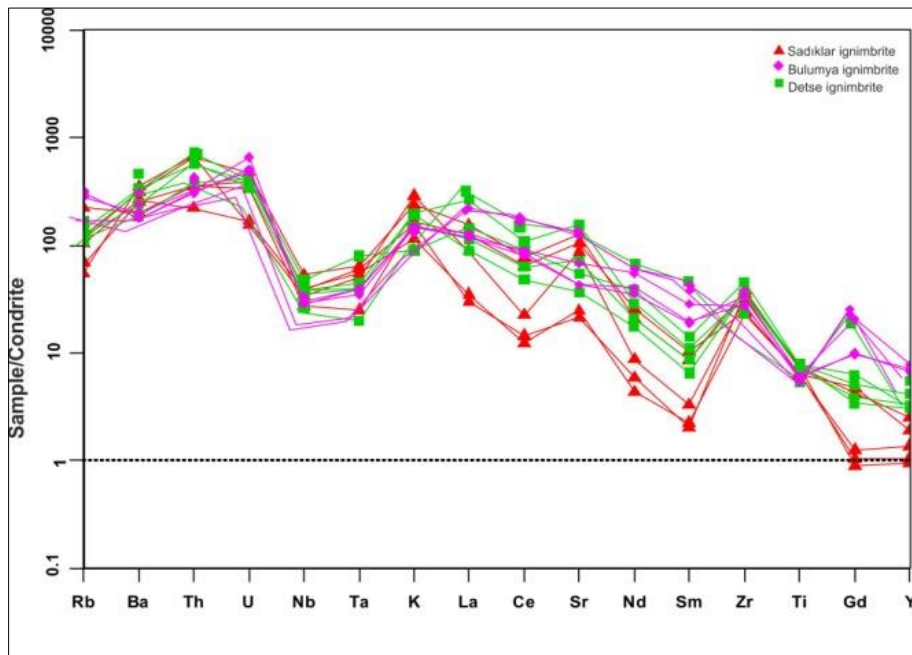


Figure 11. Examples of multi-element distributions normalized to the chondrite (Normalization values, Sun and McDonough, 1989).

Rare Earth Element Geochemistry

Values of rare earth elements of ignimbrite samples in the study area are given in Table 4. All sample distributions show parallelism with each other in the Rare Earth Element (REE) variation diagram normalized according to the chondrite of the examined samples. When the Rare Earth Element distributions were examined, it was seen that light rare earth elements (LREE) were more enriched by heavy rare earth elements (HREE). The high LREE/HREE ratios of the samples indicate an

enriched mantle source. This suggests that the magma from which the ignimbrites are derived may have been influenced by the crust. This suggests that the magma from which the ignimbrites are derived may have been affected by the crust. More pronounced Negative Eu anomaly is observed in Sadiklar and Detse samples compared to Bulumya ignimbrite. Negative Eu anomaly in Sadiklar and Detse samples indicates that plagioclase fractionation plays an important role in the development of these rocks (Figure 12).

Table 4. Rare earth element contents (ppm) of ignimbrite samples.

Samp.	La	Ce	Pr	Nd	Sm	Eu	Gd	Tb	Dy	Ho	Er	Tm	Yb	Lu
	ppm	ppm	ppm	ppm	ppm	ppm	ppm	ppm	ppm	ppm	ppm	ppm	ppm	ppm
S3	48,8	62,3	4,54	12,3	1,66	0,33	1,18	0,21	0,77	0,2	0,65	0,09	0,6	0,12
S5	11,1	10	0,76	2,6	0,43	0,05	0,29	0,04	0,25	0,09	0,24	0,03	0,26	0,03
S6	9,5	11,8	1,04	3,5	0,39	0,03	0,25	0,03	0,09	0,03	0,11	0,03	0,29	0,05
S7	28	18,2	1,56	5,2	0,63	0,12	0,35	0,05	0,38	0,05	0,14	0,04	0,26	0,04
S9	40,5	52,8	5,21	15,3	1,99	0,49	1,34	0,18	0,7	0,13	0,51	0,07	0,49	0,08
D2	35,9	51,4	4,28	12,5	1,66	0,27	1,07	0,18	0,78	0,26	0,77	0,12	0,93	0,17
D3	84,4	88,7	5,71	17,2	2,12	0,37	1,42	0,22	1,35	0,36	0,98	0,16	1,25	0,2
D5	45,9	74,4	7,42	23,1	2,7	0,54	1,76	0,24	1,35	0,24	0,72	0,13	0,76	0,13
D6	28,1	39,2	3,17	10,5	1,25	0,21	0,95	0,15	1,04	0,21	0,78	0,11	0,76	0,16
D8	178,4	339,2	37,97	128,8	16,58	3,09	10,11	0,88	3,32	0,41	1,2	0,16	0,96	0,17
B2	38	66,1	6,84	21,2	3,64	0,95	2,72	0,46	2,64	0,5	1,52	0,24	1,82	0,26
B3	143	284	32,4	125	18,5	4,19	13,7	1,33	5,8	0,79	2,21	0,24	1,37	0,2
B4	40,6	70,2	7,1	24,2	3,79	0,99	2,83	0,46	1,98	0,47	1,45	0,22	1,46	0,25
BI6	137,7	272,8	30,86	120,5	17,52	3,74	12,37	1,39	5,49	0,89	2,25	0,33	2,04	0,25
BI8	37,5	73,4	8,2	33	5,49	1,79	5,77	0,99	5,31	1,2	3,31	0,55	3,49	0,55
P1	27,7	44,5	4,38	14,6	2,42	0,72	2,5	0,45	2,59	0,54	1,76	0,27	1,86	0,32
P2	27,2	45,5	3,97	12,3	1,73	0,39	1,25	0,22	1,15	0,26	0,83	0,13	1,07	0,14

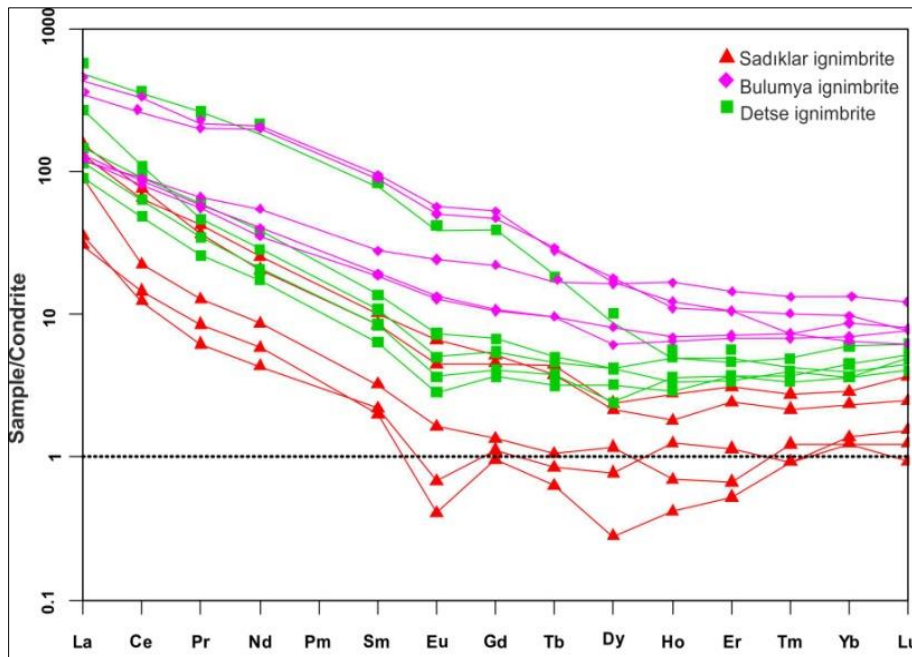


Figure 12. Rare earth element distribution plots of ignimbrite samples normalized to Chondrite (Normalization values are taken from Boynton, 1984).

Source Magma Features and Crustal Contamination

Various diagrams have been prepared in order to determine which minerals play an active role during the fractional crystallization process in the magma from which the ignimbrite samples are derived. In these diagrams, fractionation of plagioclase, olivine and apatite is observed in the samples with incompatible elements that are

enriched in the melt during the fractional crystallization process. Their ratios to each other are known to remain constant. It is possible to determine which subplate enrichment and/or crustal contamination and in-plate enrichments are effective in developing igneous rocks with diagrams using trace element ratios such as Th/Y, Nb/Y and Rb/Y. The RbY-Nb/Y diagram was created to determine the origin of the main magma for the ignimbrite samples. In the Rb/Y-Nb/Y diagram, the

Rb/Nb=1 line shows intraplate enrichments, while the vertical variation shows subduction zone enrichments and/or crustal contamination (Edwards et al., 1991). The ignimbrite samples

placed in this diagram show a vertical distribution (Figure 11b). This suggests that the magma source forming the ignimbrite samples is enriched by subduction and/or crustal components (Figure 13).

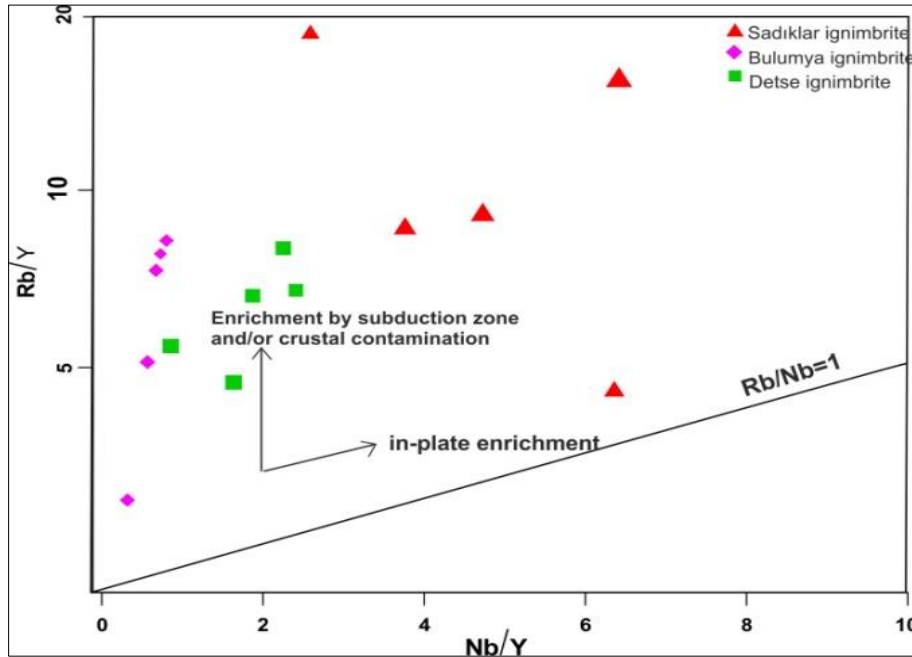


Figure 13. Nb/Y versus Rb/Y (Edwards et al., 1991) variation diagrams of ignimbrite specimens.

4. CONCLUSIONS

The study area is basically Upper Miocene - Lower Pliocene aged Güneydere formation and overlying Bulumya ignimbrite, Detse ignimbrite, Sadıklar ignimbrite and Quaternary alluviums. All these units were formed in the Upper Miocene - Lower Pliocene aged fluvial and lake environment and have a lateral vertical transition with carbonate and clastic units. The grey-colored Bulumya ignimbrite contains andesite-dacite rock fragments and large pumice grains. The Detse ignimbrite is yellow in colour and shows a well-sorted lapilli tuff composition. The Sadıklar ignimbrite contains agglomeratic levels with yellow-coloured, slightly fused lenses and wedge geometry. All ignimbrite samples have porphyritic texture and were classified as “crystal-vitric tuff” and “crystal lithic-vitric tuff” in the glass-crystal-rock fragment classification. In petrographic investigations of ignimbrites, general mineral paragenesis consists of quartz, plagioclase, plagioclase microliths, biotite, muscovite, amphibole, opaque minerals and rock fragments. When geochemical data are evaluated, it is observed that all ignimbrite samples are sub-alkaline, trachy-andesite, andesite-basaltic andesite and calc-alkaline in character. When the primary mantle and chondrite normalized spider diagrams are examined, a significant lithophile element enrichment with a large ion radius and significant negative anomaly in elements with high persistence and depletion in REEs are observed. When the Rare Earth Element distributions were examined, it was

seen that light rare earth elements (LREE) were more enriched by heavy rare earth elements (HREE). The high LREE/HREE ratios of the samples indicate an enriched mantle source. In addition, the high K and Rb content in the spider diagrams indicate shell contamination. The Rb/Y-Nb/Y diagram suggests that the magma source constituting the ignimbrite samples is enriched by subduction and/or crustal components.

Acknowledgement

The author is indebted to the anonymous reviewers and the editors for their valuable and constructive suggestions.

Author Contributions

Hacer Bilgilioğlu: Methodology, Validation, Formal analysis, Writing-Original Draft, Writing- Reviewing and Editing, Visualization. **Halil Baş:** Conceptualization, Methodology.

Conflicts of Interest

The authors declare no conflict of interest.

REFERENCES

Asan, K., & Erturk, M.A. (2013). First Evidence of Lamprophyric Magmatism from the Konya Region, Turkey: a Genetic Link to High-K

- Volcanism. *Acta Geologica Sinica-English Edition*, 87(6), 1617-1629.
- Boynton, W.V. (1984). Cosmochemistry of the rare earth elements: meteorite studies. In *Developments in geochemistry* (Vol. 2, pp. 63-114). Elsevier.
- Carozzi, A.V. (1993). *Sedimentary Petrography*: PTR Prentice Hall. Inc. Nova Jersey.
- Cas, R.A.F., & Wright, J.V. (1988). An Introduction to facies analysis in volcanic terrains. *Volcanic Successions Modern and Ancient: A geological approach to processes, products and successions*, 2-12.
- Edwards, C., Menzies, M., & Thirlwall, M. (1991). Evidence from Muriah, Indonesia, for the interplay of supra-subduction zone and intraplate processes in the genesis of potassic alkaline magmas. *Journal of petrology*, 32(3), 555-592.
- Eren, Y. (1993). Konya kuzeybatısında Bozdağlar masifinin otokton ve örtü birimlerinin stratigrafisi. *Türkiye jeoloji bülteni*, 36(2), 7-23.
- Eren, Y. (1993), The Geology of the Eldeş-Derbent-Tepeköy-Söğütözü (Konya) region (PhD thesis). Selçuk University. Konya, Turkey (in Turkish).
- Göğer, E., & Kırıl, K. (1973). Kızılören dolayının (Konya'nın batısı) genel stratigrafisi. MTA Rapor, (5204).
- Irvine, T.N., & Baragar, W.R.A. (1971). A guide to the chemical classification of the common volcanic rocks. *Canadian journal of earth sciences*, 8(5), 523-548.
- Keller, J., Jung, D., Burgath, K., & Wolff, F. (1977). Geologie und Petrologie des neogenen Kalkalkali-Vulkanismus von Konya (Erenler Dag-Alaca Dag-Massiv, Zentral-Anatolien).
- Kempler, D., & Garfunkel, Z. (1991). The northeast Mediterranean triple junction from a plate kinematics point of view. *Bull. Tech. Univ. Istanbul*, 44(spec. issue), 425-454.
- Koçak, K. (2012). Geochemical characteristics of the Late Miocene to Pliocene Ulumuhsine sill of the Erenlerdagi volcanics, Konya, Central Turkey. School «Geochemistry of Alkaline rocks» Ore potential of alkaline, kimberlite and carbonatite magmatism, 2012, 14-18 September, Sudak, Ukraine.
- Koçak, K. (2017). Geochemical Characteristics of the Mafic Enclaves and Their Hosts from Neogene Erenlerdagi Volcanites, around Yatagan Village and Sağlık Town (Konya), Central Turkey. *Bulletin of the Geological Society of Greece*, 50(4).
- Kocak, K. (2021). Geological Characteristics of The Neogene Volcanic Plugs in Inlice (Konya) Area, Central Turkey Proceedings 2021.
- Kocak, K., & Kaya, R.M. (2019). Chemical and Mineralogical Characteristics of the Microscopic-sized Epidotes in the Metamorphic Basement Rocks within the Late Cretaceous Hatip Ophiolitic Melange in Konya (Central Southern Turkey). *Hittite Journal of Science and Engineering*, 6(3), 167-172.
- Kurt, H., Özkan, A.M., & Kocak, K. (2003). Geology, Petrography And Geochemistry Of The Subduction Related Volcanic Rocks, West Of Konya, Central Anatolia. *Türkiye Jeoloji Bülteni*, 46(2), 39 – 51.
- Marshall P. (1935). Acid rocks of Tanpo-Rotorua volcanic district. *Trans., R. Soc. N.Z.*, 64.. 323-375.
- McKenzie, D. (1972). Active tectonics of the Mediterranean region. *Geophysical Journal International*, 30, 109-185.
- McKenzie, D., & Yılmaz, Y. (1991). Deformation and volcanism in western Turkey and the Aegean. *Bulletin of the Technical University of Istanbul*, 44(1-2), 345-373.
- McPhie, J. (1993). Volcanic textures: a guide to the interpretation of textures in volcanic rocks.
- Ota R. & Dinçel A. (1975). Volcanic rocks of Turkey *Bull. Geol. Surv. Jpn.*, 26, pp. 19-45.
- Özcan, A., Göncüoğlu, M.C., Turhan, N., Şentürk, K., Uysal, S., & Işık, A. 1990. Konya – Kadınhanı – Ilgın dolayının temel jeolojisi ; M.T.A. rap. 736, Konya.
- Pearce, J. (1996). Sources and settings of granitic rocks. *Episodes Journal of International Geoscience*, 19(4), 120-125.
- Pearce, J.A., Harris, N.B., & Tindle, A.G. (1984). Trace element discrimination diagrams for the tectonic interpretation of granitic rocks. *Journal of petrology*, 25(4), 956-983.
- Peccerillo, A., & Taylor, S.R. (1976). Geochemistry of Eocene calc-alkaline volcanic rocks from the Kastamonu area, northern Turkey. *Contributions to mineralogy and petrology*, 58, 63-81.

- Rollinson, H.R. (1993). Using geochemical data: Evaluation, presentation, interpretation. John Wiley & Sons Inc., New York. 352pp.
- Schmid, R. (1981). Descriptive nomenclature and classification of pyroclastic deposits and fragments: Recommendations of the IUGS Subcommittee on the Systematics of Igneous Rocks. *Geologische Rundschau*, 70, 794-799.
- Şengör, A.M.C., Görür, N., & Şaroğlu, F. (1985). Strike-slip faulting and related basin formation in zones of tectonic escape: Turkey as a case study.
- Soğucaklı Ö., (2006). The Geology of Hatunsaray - Çatören district (Western Konya), (MSc thesis). Selçuk University, Konya, Turkey (in Turkish).
- Sparks, R.S.J., Self, S., & Walker, G.P. (1973). Products of ignimbrite eruptions. *Geology*, 1(3), 115-118.
- Sun, S.S., & McDonough, W.F. (1989). Chemical and isotopic systematics of oceanic basalts: implications for mantle composition and processes. *Geological Society, London, Special Publications*, 42(1), 313-345.
- Temel, A., Çelik, M., & Tunoğlu, C. (1995). Konya batı-güneybatısında yer alan Neojen yaşlı volkanosedimanter basenindeki kil oluşumları. *In VII National Clay Symposium* (pp. 32-45).
- Temel, A., Gündoğdu, M.N., Gourgaud, A., & Le Pennec, J.L. (1998). Ignimbrites of Cappadocia (central Anatolia, Turkey): petrology and geochemistry. *Journal of Volcanology and Geothermal Research*, 85(1-4), 447-471.
- Turan, A., Küpeli, Ş., & Karakoç, İ. (1997). Loras Dağı-Çaldağı ile Hatunsaray (Konya batısı) arasında kalan bölgenin stratigrafisi ve bazı tektonik özellikleri. *Geosound*, 1(30), 305-318.
- Ulu, Ü., Öcal, H., Bulduk, A.K., Karakaş, M., Arbas, A., Saçlı, L., & Karabıyıkoglu, M. (1994). Cihanbeyli-Karapınar yöresi geç Senozoyik çökeltme sistemi: Tektonik ve iklimsel önemi. *Türkiye Jeoloji Kurultayı Bülteni*, 9, 149-163.
- Uyanık, C., & Koçak, K. (2016). Geochemical Characteristics of the Erenlerdağı Volcanics, Konya, Central Turkey. *Bulletin of the Geological Society of Greece*, 50(4), 2057-2067.



© Author(s) 2021. This work is distributed under <https://creativecommons.org/licenses/by-sa/4.0/>